Analyses of truncated fibrillin caused by a 366 bp deletion in the *FBN1* gene resulting in Marfan syndrome

Michael RAGHUNATH,*|| Cay M. KIELTY,† Katariina KAINULAINEN,‡ Anne CHILD,§ Leena PELTONEN‡ and Beat STEINMANN*

*Division of Metabolism, Department of Paediatrics, University of Zürich, CH-8032 Zürich, Switzerland, †School of Biological Sciences, Division of Biochemistry, University of Manchester, Manchester, U.K., ‡NPHI, Department of Human Molecular Genetics, Helsinki, Finland, and §St. George's Hospital, London, U.K.

We studied fibrillin synthesis in cultured fibroblasts from 11 members of a three-generation family with Marfan syndrome, caused by a large in-frame deletion in *FBN1* (the fibrillin gene) leading to a loss of 366 bases in the corresponding fibrillin mRNA. Metabolic labelling with [^{35}S]Met/Cys and SDS/PAGE allowed unequivocal identification of normal and truncated fibrillin in all cell strains harbouring the deletion. In culture medium, fibrillin and its truncated counterpart were predominant, whereas their respective larger precursors were found only in traces. This proportion, however, was markedly shifted towards the normal and truncated precursors by EGTA and reversed by the addition of calcium, which confirmed the existence of profibrillin and its probably calcium-dependent conversion into fibrillin. Tunicamycin caused increased electrophoretic mobility of normal and truncated molecules without changing their apparent size differences. Intracellularly, only profibrillin was found; in the mutant cells truncated and normal profibrillin molecules were present in similar amounts and both populations were secreted and deposited simultaneously into the extracellular matrix; there, however, truncated profibrillin only became easily detectable after treatment of cells with dextran sulphate, which increased the amount of extractable profibrillin. Immunofluorescence microscopy in patients' cultures identified fibrillin-containing microfibrils which appeared to be moderately reduced both in amount and diameter. Ultrastructural analysis by rotary-shadowing and immunogold electron microscopy demonstrated the presence of numerous beaded domains reacting with fibrillin antibodies, but no intact fibrillin microfibrils in patient's cell-layer extracts, in contrast with the extensive microfibrils elaborated by control cultures. Our findings suggest, that in the patients' cell cultures all microfibrils contained the truncated fibrillin molecules.

INTRODUCTION

Marfan syndrome (MFS) is an autosomal dominant connective-tissue disorder characterized by cardiovascular, ocular and skeletal manifestations [1]. It is caused by a deficiency of fibrillin (Fib), a major constituent of microfibrils in the extracellular matrix (ECM) [2,3]. The coincident assignment of MFS to chromosome 15q21 by linkage analyses [4,5] and localization of the gene coding for Fib, *FBN1*, to the same locus using *in situ* hybridization [6] were complemented by identification of the first (point) mutation in two unrelated MFS patients of the Fib-specific cDNA [7], which has been fully sequenced recently [8]. Further, at least five *FBN1* mutations predicting shortened Fib polypeptide chains have been published [9–12]. One of them is a large in-frame deletion resulting in a loss of 366 bases in the respective mRNA (Figure 1). This mutation co-segregates with the disorder in a three-generation MFS family and, as reported earlier [9], immunoprecipation experiments led to the observation of a truncated fibrillin (Fib′) in the medium of cultured fibroblasts of family member II/2 (Figure 2). Here we have extended this study to 11 members of this family in order to demonstrate co-segregation of the mutation at the protein level and to use the truncated molecules to study the post-translational processing of Fib and its precursor proFib. The impact of this mutation on Fib assembly in the ECM has also been investigated.

MATERIALS AND METHODS

Subjects

The composite phenotype of the affected individuals from the three-generation British family (Figure 2) is characterized by a moderately marfanoid habitus with mild scoliosis and hypermobility of both large and small joints in the absence of ectopia lentis. Lattice degeneration of the retina was known in I/1, II/2 and II/3. Aortic root dilatation was present in 0/1 (late dissection at the age of 56 years), in II/2, II/3 and II/6. Another feature in this family is mitral-valve prolapse, with associated arrhythmia requiring β-blocker therapy in II/3 and II/6, and surgical replacement of the mitral valve in II/6 at age 32 years. This affected member developed progressive cardiac dilatation and chronic heart failure and died at 44 years of age of acute ventricular arryhthmia while awaiting cardiac transplant. In the third generation mitral-valve prolapse has been diagnosed in members III/4, III/6, III/7 and III/8. However, because of the mild phenotype and the young age of the members of the third generation, clinical diagnosis was uncertain in members III/1, III/2, III/3 and III/6, III/7, III/8. In contrast, family member III/9 was clearly unaffected. His dermal fibroblasts and a culture from a healthy unrelated individual were used as intra- and extra-familial controls respectively.

Abbreviations used: MFS, Marfan syndrome; Fib, fibrillin; Fib′, truncated Fib; proFib, profibrillin; proFib′, truncated profibrillin; *FBN1*, fibrillin gene on chromosome 15; ECM, extracellular matrix; EM, electron microscopy; FCS, fetal-calf serum; MSH, mercaptoethanol; MEM, minimal essential medium; NP-40, Nonidet P-40; PMSF, phenylmethanesulphonyl fluoride; RT, room temperature; HBSS, Hanks' balanced salt solution.

|| To whom correspondence should be addressed.

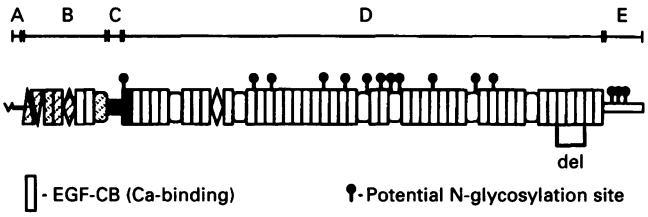

Figure 1 Domain model of Fib deduced from the *FBN1* cDNA sequence (adapted from [8])

This model illustrates the modular composition of the Fib molecule encoded by the *FBN1* gene on chromosome 15. The 366 bp deletion in the mRNA resides close to the C-terminal end of region D and results in the loss of three entire EGF-CB repeats (122 residues) as indicated by 'del'. The pins on top of the module symbols designate the 15 potential N-glycosylation sites, 11 of which are present in region D and three of which are concentrated in region E, the Fib-specific C-terminus.

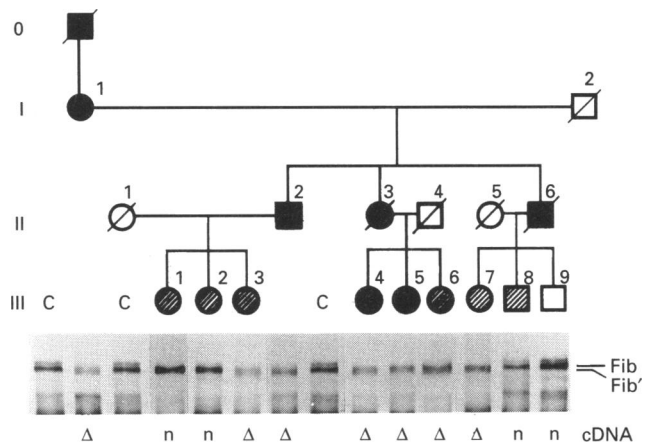

Figure 2 Pedigree of the MFS family and the corresponding genotype and chemotype

Closed symbols indicate affected individuals, open symbols unaffected ones, and possibly affected members are indicated by hatched symbols. Individuals not examined are marked by (/) and the unrelated control subject by C. The lowest panel shows the cDNA findings and designates the family members either as normal (n) or as carrier of the *FBN1* deletion which is symbolized by the Δ. The centre panel displays the Fib chemotype as secreted by fibroblasts into culture medium during a 4 h pulse, as revealed by SDS/PAGE and fluorography. Note the narrow doublet in all members carrying the *FBN1* deletion (Δ) resulting from Fib and the faster-migrating Fib, whereas healthy family members and the external control [C] express the wild type only.

Mutation identification

Total RNA was extracted from cultured skin fibroblasts [13] and first-strand cDNA was synthesized from 1 μg of total RNA using 20 units of AMV reverse-transcriptase enzyme (Promega) and a primer corresponding to nucleotides 5′-8727–8703-3′ of Fib cDNA [8]. One-tenth of the synthesized cDNA was used as a template to amplify with primers flanking the deletion, namely 5′-7164–7183-3′ and 5′-7955–7933-3′ [8], resulting in a fragment of 792 bp representing the normal allele and a fragment of 426 bp representing the mutated allele. cDNA synthesis, PCR and detection of the mutation was performed as described elsewhere in detail [9].

Quantification of the ratio of normal and mutant RNA in fibroblasts of affected family members

To assess the ratio of normal and mutant RNA synthesized by fibroblasts of I/1 and II/2, a PCR reaction to detect the deletion was performed in a total volume of 100 μl and samples of 10 μl were taken after 5, 10, 15, 20, 25 and 30 PCR cycles. The samples were run on a 1% (w/v) agarose gel. Transfer to a Hybond-N nylon membrane, prehybridization and hybridization of the filter using the probe for Fib (CLM-5, a probe covering nucleotides 4322–8496 of the Fib cDNA [8]) were performed according to standard procedures. The intensity of the signals were determined by optical scanning of the X-ray film and the ratio was determined from the linear part of the curve for both transcript types separately.

Metabolic labelling

Cells (1×10^5) were seeded in 15-mm-diam. dishes (4-well dishes Nunclon, 1.8 cm^2) in minimal essential medium (MEM) (Gibco) with 10% (v/v) fetal-calf serum (FCS), 5 mM glutamine and antibiotics. The next day (day 2) the medium was removed, the cells were washed twice and incubated for 30 min in MEM lacking methionine, cysteine and FCS ($MEM^-/^-/^-$; Northumbria), and finally pulsed with 25 μCi of TranSlabel [^{35}S]Met/Cys (ICN) in 200 μl of $MEM^-/^-/^-$ for 4 h. For pulse–chase experiments the cells were depleted on day 3, and pulsed for 30 min with 50 μCi of TranSlabel in 200 μl of $MEM^-/^-/^-$. The pulse medium was removed, the cells washed twice with complete MEM and chased with 200 μl of MEM containing 5 mM glutamine, 1% (v/v) FCS, 10 mM Met and 1 mM Cys. The chase times were 0, 0.5, 1, 2, 4, 24 and 51 h. In some experiments the following substances were added to the chase medium in the respective final concentrations: 0.01% dextran sulphate (Fluka), a mixture of 1 mM each of phenylmethanesulphonyl chloride/*N*-ethylmaleimide (Sigma), a mixture of 1 mM each of *N*-tosyl-L-lysine-chloromethane hydrochloride/tosylphenylalanine-chloromethane, 1 mM leupeptin (Sigma), and 0.5 mM E-64 [l-*trans*-epoxysuccinyl-leucylamide(4-guanidino)butane, Fluka], a specific cysteine proteinase inhibitor. In these experiments 70 μCi of TranSlabel were used.

Immunoprecipitation of Fib

Cells (1×10^6) from of III/4 and the extrafamilial control were seeded in 35-mm-diam. dishes. They were pulsed the next day for 4 h with 50 μCi of TranSlabel in 500 μl of $MEM^-/^-/^-$. Media and cell lysates were harvested into separate Eppendorf tubes containing 50 μl of 1 M Tris/HCl, pH 7.4. The samples were incubated for 1 h at room temperature (RT) on an overhead rotator with 30 μl of normal rabbit serum; then 50 μl of Protein A–Sepharose (Sigma; 4 g swollen in 6 ml of Tris buffer) and 50 μl of gelatine–Sepharose (Pharmacia) were added and samples incubated for another hour. The beads were sedimented using a microfuge (MSE Scientific Instruments) and supernatants were transferred to fresh Eppendorf tubes. We used a specific polyclonal antibody to Fib, 5507, which had been raised in rabbits to whole microfibril preparations from skin [14]. Aliquots (20 μl, 10 μl and 5 μl) were added to each 500 μl sample of control and III/4 respectively. As a control, 20 μl of normal rabbit serum were used. Incubation was overnight at 7 °C. Samples were then allowed to reach RT and 50 μl of a suspension of Protein A–Sepharose beads were added. After incubation for 1 h at RT, the beads were washed twice for 20 min with RIPA-buffer [50 mM Tris, pH 7.5, 150 mM NaCl, 1% Nonidet P-40 (NP-40), 0.5% desoxycholate, 0.1% SDS] and once for 20 min

with 10 mM Tris/0.1% NP-40. Bound Fib was recovered by heating the beads in 50 μl of double-strength sample buffer containing 20% (v/v) mercaptoethanol (MSH) and 1 M urea for 5 min at 100 °C in a heating block (Liebisch).

Inhibition of N-linked glycosylation

Cells from the external control and I/1 were continuously pulsed for 16 h with 25 μCi of TranSlabel in 200 μl of MEM^{-}/$^{-}$/$^{-}$ containing 5 μg/ml tunicamycin (Fluka); only the media were processed for SDS/PAGE.

Precursor relationship of proFib and Fib

Cells from the external control and III/4 were continuously pulsed for 4 h with 50 μCi of TranSlabel in 200 μl of MEM^{-}/$^{-}$/$^{-}$ in the presence of 5 mM EGTA, 5 mM EGTA plus 5 mM $CaCl_2$ or without additives. Only media were processed for SDS/PAGE. As an experimental control, medium from pulsed cells without the above-mentioned additives was combined with sample buffer as described and then EGTA or EGTA/$CaCl_2$ were added shortly before boiling.

Processing of samples for SDS/PAGE analysis of radiolabelled Fib

The medium (200 μl) was aspirated and added to 200 μl of double-strength sample buffer [15] supplemented with urea and an additional 40 μl of MSH (final concentrations 0.5 M and 10% respectively). The wells were washed twice with ice-cold Hanks' balanced salt solution (HBSS) lacking Ca^{2+}/Mg^{2+}, and the cells lysed in 200 μl of 10 mM Hepes, pH 7.4, containing 1 mM EGTA, 1% NP-40, 1 mM phenylmethanesulphonyl fluoride (PMSF) and 1 mM *N*-ethylmaleimide for 10 min on ice. The cell lysate was transferred to modified Laemmli buffer as described. The remainder in the dish, i.e. ECM by definition, was washed twice with HBSS and extracted with 440 μl of normal-strength sample buffer (0.5 M urea and 10% MSH) for 10 min at RT. The samples were boiled for 3 min, centrifuged and 30 μl of each used for 4%/7% step-gel SDS/PAGE as described in detail [16]. The gels were then processed for fluorography [17].

Immunofluorescence studies

Cells (1×10^6 per 35-mm-diam. dish) were grown on glass coverslips for 72 h to hyperconfluency and fixed in methanol for 10 min at −20 °C and air-dried. The monolayers were rehydrated and unspecific binding sites blocked in PBS/1% BSA/10% normal goat serum for 30 min, the blocking solution was drained off and replaced by monoclonal antibody anti-Fib F2 (a generous gift from Dr. Maurice Godfrey, Omaha, NE, U.S.A.) diluted 1:15. The solution was incubated overnight at 7 °C. A Texas-Red-coupled goat anti-(mouse IgG) antibody (Jackson Immunoresearch), diluted 1:50 in PBS/BSA and applied for 30 min at RT, was used to detect bound specific antibody. The coverslips were mounted in Mowiol (Hoechst) and photographs at fixed exposure times were taken on Ilford HP 5 plus film using Polyvar (Reichert-Jung) epifluorescence equipment.

Microfibril extraction from cell culture and processing for rotary-shadowing electron microscopy (EM)

Cells were maintained at post-confluence for up to 3 weeks. For microfibril extractions, cell layers were washed in 0.05 M Tris/HCl, pH 7.4 containing 0.4 M NaCl (Tris/saline), and digested for 3 h at 20 °C with 0.1 mg/ml bacterial collagenase (type 1A; Sigma) in Tris/saline supplemented with 5 mM $CaCl_2$, 2 mM PMSF and 5 mM *N*-ethylmaleimide. Soluble extracts were clarified by centrifugation for 15 min at 7500 ***g*** in a bench microfuge. The extracts were chromatographed directly without concentration under non-reducing, non-denaturing conditions on a Sepharose CL-2B column equilibrated and eluted at RT with Tris/saline [18]. High-molecular-mass material present in the excluded volume was retained and visualized for its microfibril content by rotary-shadowing EM using a modification of the mica sandwich technique [19]. Immunogold EM of Fib microfibrils was carried out with polyclonal rabbit antibody 5507 raised to Fib, as recently described [20].

RESULTS

Mutation identification

As summarized in Figure 2, amplification of the Fib-specific cDNA revealed that the cells of the clearly affected members I/1, II/2, III/4 and III/5 synthesized both normal and mutant mRNA species for Fib. In the clinically uncertain cases, the 366 bp deletion was detected in III/3, III/6 and III/7, whereas it was excluded in III/1, III/2, III/8, as well as in the unaffected individual III/9. The normal and shortened transcripts were found in equal amounts in the fibroblasts of MFS patients. The obtained result is based on the assumption that the reverse-transcriptase reaction was equally efficient in the case of both mRNA species.

Identification of Fib by radioimmunoprecipitation

Polyclonal antibody 5507 to Fib precipitated a ^{35}S-labelled protein with a molecular mass of about 320 kDa and traces of a larger proform of about 350 kDa from culture medium of the control (Figure 3). The mixture of normal and truncated fibrillin molecules in patient III/4 was evident by a broader Fib band, containing a faster-migrating population. A few smaller-molecular-mass proteins could be identified as non-specific because they were also recovered with normal rabbit serum. Only the wild-type and truncated proforms were immunoprecipitable, albeit in poor yield, from cell lysates of control and III/4 respectively (results not shown).

Findings at the protein level: short pulse studies for diagnostic use

The 4-h-long pulse protocol and SDS/PAGE of the culture media allowed us to obtain first results 50 h after seeding the cells. In all fibroblast cultures of the family members carrying the deletion, Fib appeared as a narrow doublet representing the gene products from both alleles in similar amounts, i.e. Fib and Fib′ (Figure 2). We thus could definitely classify the 11 members analysed at the protein level as either affected or not affected; in the third generation protein analysis was done without previous knowledge of the cDNA data, in four cases the results were obtained before cDNA analysis. The cDNA analyses were in complete agreement with the protein analyses and the individuals carrying the deletion could be unequivocally identified (Figure 2).

Findings at the protein level: pulse–chase studies

Cell lysates

The 4/7% step gels allowed quantification of radiolabelled proFib of approx. 350 kDa relative to that of the 57 kDa

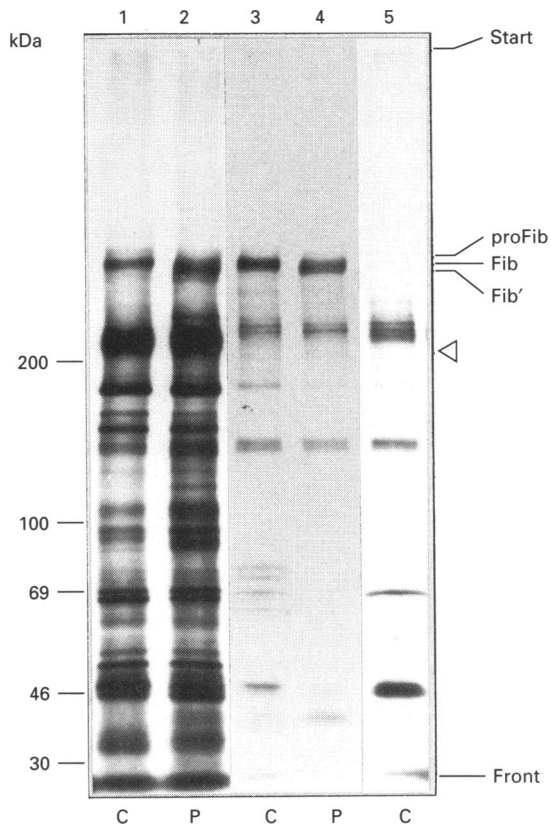

Figure 3 Identification by radioimmunoprecipitation of wild-type and truncated fibrillin from medium of cultures of control (C) and of patient III/4 (P) with MFS

Fibroblasts were pulsed for 4 h with [^{35}S]Met/Cys and culture medium and intracellular proteins harvested separately. Fib was isolated by immunoprecipitation with 20 μl of polyclonal rabbit antiserum 5507 and electrophoresed under reducing conditions by SDS/PAGE. The open arrowhead indicates the transition between 4% and 7% layers of the step gel. Lanes 1 and 2 contain the total proteins secreted into culture medium by cells of the control (C) and III/4 (P) with MFS. Lanes 3 and 4 are immunoprecipitates with 20 μl of antibody 5507. Lane 5 represents material precipitated with a non-specific rabbit antiserum from control medium. Fib is immunoprecipitated as a single band from culture medium of control cells, whereas an additional faster-migrating population produced by the patient's cells causes downwards broadening of the corresponding band. The larger precursor proFib is faintly visible in lane 3. Other smaller-molecular-mass bands are clearly attributable to background as compared with lane 5 which is over-exposed with respect to the other lanes to show absence of specific bands. Molecular masses are indicated at the left margin.

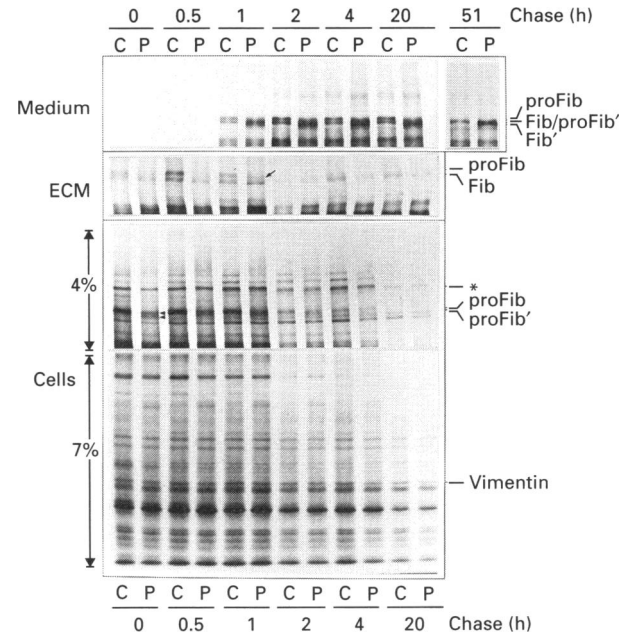

Figure 4 Pulse–chase metabolic labelling and SDS/PAGE analysis of Fib from cultures of control (C) and of patient III/4 (P) with MFS

In order to demonstrate simultaneous resolution of both proFib/Fib and vimentin (57 kDa) a fluorogram of a full-length 4/7% step gel is given for the cell lysates (Cells), whereas only the truncated parts of the 4% step are given for the ECM extracts (ECM) and the culture media (Medium). Cell lysate: early chase times reveal the presence of both proFib and the truncated counterpart proFib′ in the patient (P), which form a narrow doublet (arrowheads). There is no evidence for delayed biosynthesis or retention of the shortened chain. The asterisk indicates a band of an anonymous protein in the cell lysate [23] serving as additional internal marker. ECM: proFib and Fib chains in the control are visible only during the first 2 h of chase. The patient's cells show reduced amounts of normal proFib, whereas a putative proFib′ is faintly visible at 1 h chase (arrow). Medium: Up to 20 h proFib and Fib are discernible in the controls. In P representing proFib, proFib′, Fib and Fib′ results in a blurred quadruplet. Unlike in the ECM, the proportions of proFib and Fib remain stable for up to 20 h. In a separate 51 h chase experiment both normal and shortened proFib are no longer visible.

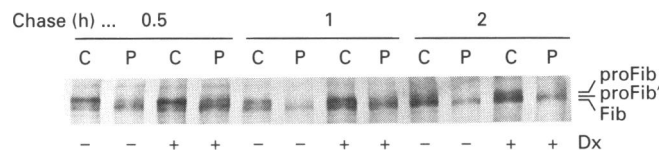

Figure 5 Pulse–chase study of ECM in the absence or presence of 0.01% dextran sulphate (Dx)

The apparent conversion of proFib into Fib in the control (C) appears markedly slowed by Dx and, in addition, more proFib and Fib is extractable from the ECM and the specific bands persist for a longer time. In the patient (P) the primarily deposited amount of normal proFib is markedly reduced. Dx enhances detection of a band migrating between proFib and Fib which represents the truncated proFib′.

intermediate filament protein vimentin [21] which served as internal standard for the cell mass [16]. Vimentin was simultaneously resolved in the 7% layer and only detectable in the cell lysates (Figure 4). Control and MFS (III/4) fibroblasts synthesized comparable amounts of Fib and fibronectin. In the patient's sample two populations, proFib and the truncated proFib′, were detectable in similar amounts up to 2 h of chase. The truncated chains were secreted as the normal ones (Figure 4, lower panel).

ECM

The control showed an initial ratio of proFib/Fib of approx. 1:1, which had shifted towards Fib with only spurious amounts of proFib after 2 h chase. Less than half the amount of wild-type proFib was extractable from the patient's cell cultures in comparison with the control. In the depicted experiment, the presence of a truncated proFib at 1 h might be assumed (Figure 4, centre panel). It was, however, visible in separate experiments using 70 μCi of TranSlabel and could be enhanced in the presence of 0.01% dextran sulphate (Figure 5), but not with the proteinase inhibitors (results not shown).

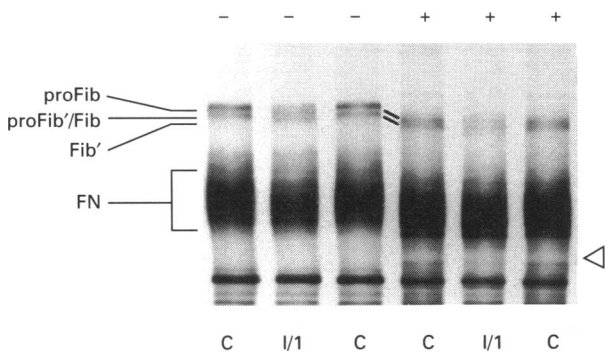

Figure 6 Inhibition of N-linked glycosylation of normal and truncated proFib/Fib in MFS fibroblasts

Cells from a control (C) and patient I/1 were pulsed with [^{35}S]Met/Cys for 16 h in the absence (−) or presence (+) of 5 μg/ml tunicamycin. The untreated control cells showed two bands, proFib and Fib, whereas I/1 displayed additionally proFib′ and Fib′ forming at least a triplet. Tunicamycin caused a markedly higher mobility of Fib and proFib by approx. 60 kDa. proFib migrated relatively faster and therefore closer to Fib. proFib and Fib of I/1 behaved similarly, however, the apparent size difference to their truncated counterparts remained unchanged. The several fibronectin (FN) bands migrate faster, as well. The open arrowhead indicates the border between the 4% and 7% layer of the step gel.

Culture media

SDS/PAGE analysis of the medium of control fibroblasts showed, after a 1 h chase, appearance of Fib at approx. 320 kDa and a weaker signal from the larger precursor 'proFib' (compare also with Figures 2, 3 and 4). The initial ratio of proFib/Fib varied from experiment to experiment but remained stable within a given experiment for up to 20 h chase time. After a prolonged chase time (51 h), however, proFib vanished leaving Fib as the only band (Figure 4, top panel). The patient's fibroblasts showed Fib and Fib′ and only minimal amounts of normal proFib. proFib migrated almost with normal Fib and could not be resolved as a separate band between proFib and Fib (Figure 4, top panel) resulting in a blurred triplet or a quadruplet of bands. After prolonged chase, the ratio shifted towards Fib.

Effects of tunicamycin

In the controls, inhibition of N-linked glycosylation with tunicamycin caused a markedly faster migration in electrophoresis of both proFib and Fib, suggesting an apparent decrease in molecular mass of about 60 kDa. The apparent size difference, however, between the underglycosylated proFib and Fib was reduced to about 15 kDa, which was due to a relatively faster migration of proFib. The relative migrational differences (about 12 kDa) of Fib and proFib to their respective truncated counterparts in the MFS cells, however, appeared unchanged (Figure 6).

Effects of EGTA on the conversion of proFib into Fib

Whereas in normal cells the ratio of proFib:Fib appeared somewhat variable in pulse–chase experiments, it was mostly clearly in favour of Fib in 4 h pulse studies. In the presence of EGTA, this ratio was shifted markedly to proFib, depending on the rate of initial conversion in the respective experiment (Figure 7). Accordingly, EGTA caused a marked shift from the predominant Fib/Fib′ bands to proFib/proFib′ in cell strain III/4

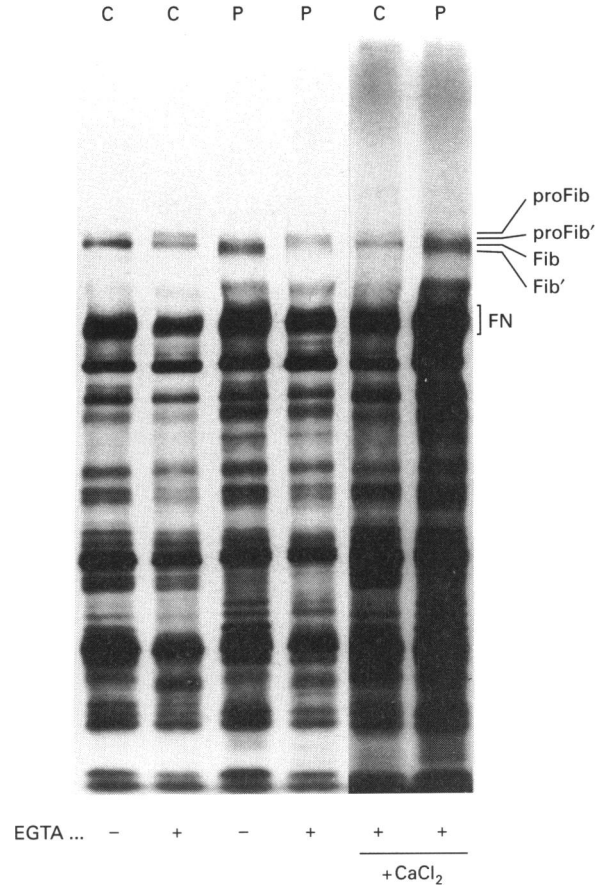

Figure 7 Preferential calcium chelation with EGTA slows conversion of proFib into Fib

A 4 h pulse with [^{35}S]Met/Cys in the presence (+) or absence (−) of 5 mM EGTA in a control (C) and patient III/4 (P). Untreated control shows a faint proFib and a pronounced Fib band. Untreated cells of P show a hardly visible normal proFib band and the pronounced doublet of Fib and Fib′, whereas proFib′ is not discernible here. In the presence of EGTA the control medium shows a marked shift to proFib. Only proFib and proFib′ and no Fib/Fib′ are visible in P. Note, that the intrinsic calcium concentration of the MEM used is 1.8 mM according to the manufacturer so that an excess of 3.2 mM EGTA results. The resupplementation of equimolar $CaCl_2$ to EGTA reversed the EGTA effect. (The respective lanes are exposed for longer but derived from the same gel).

(Figure 7). The addition of equimolar $CaCl_2$ reversed the phenomenon (Figure 7). The addition of EGTA or EGTA/$CaCl_2$ after the pulse period and transfer of the culture medium to sample buffer prior to boiling did not cause these electrophoretic shifts or any other changes. The 4 h treatment of the cells with EGTA caused neither detachment nor significant impairment of biosynthesis and secretion of proFib. However, when we used a cell-permeable form, EGTA-AM (Calbiochem), a marked biosynthetic and secretory shut down of proFib and other proteins occurred (results not shown). The addition of $CaCl_2$ led to a reduced incorporation of label and rounding of the cells. The other proteinase inhibitors did not have any effects on the relative amounts of proFib and Fib.

Morphological studies

Anti-Fib immunofluorescence revealed microfibrils accumulated to a meshwork in normal hyperconfluent fibroblast cultures (Figure 8a). In two affected members (only III/4 shown) the

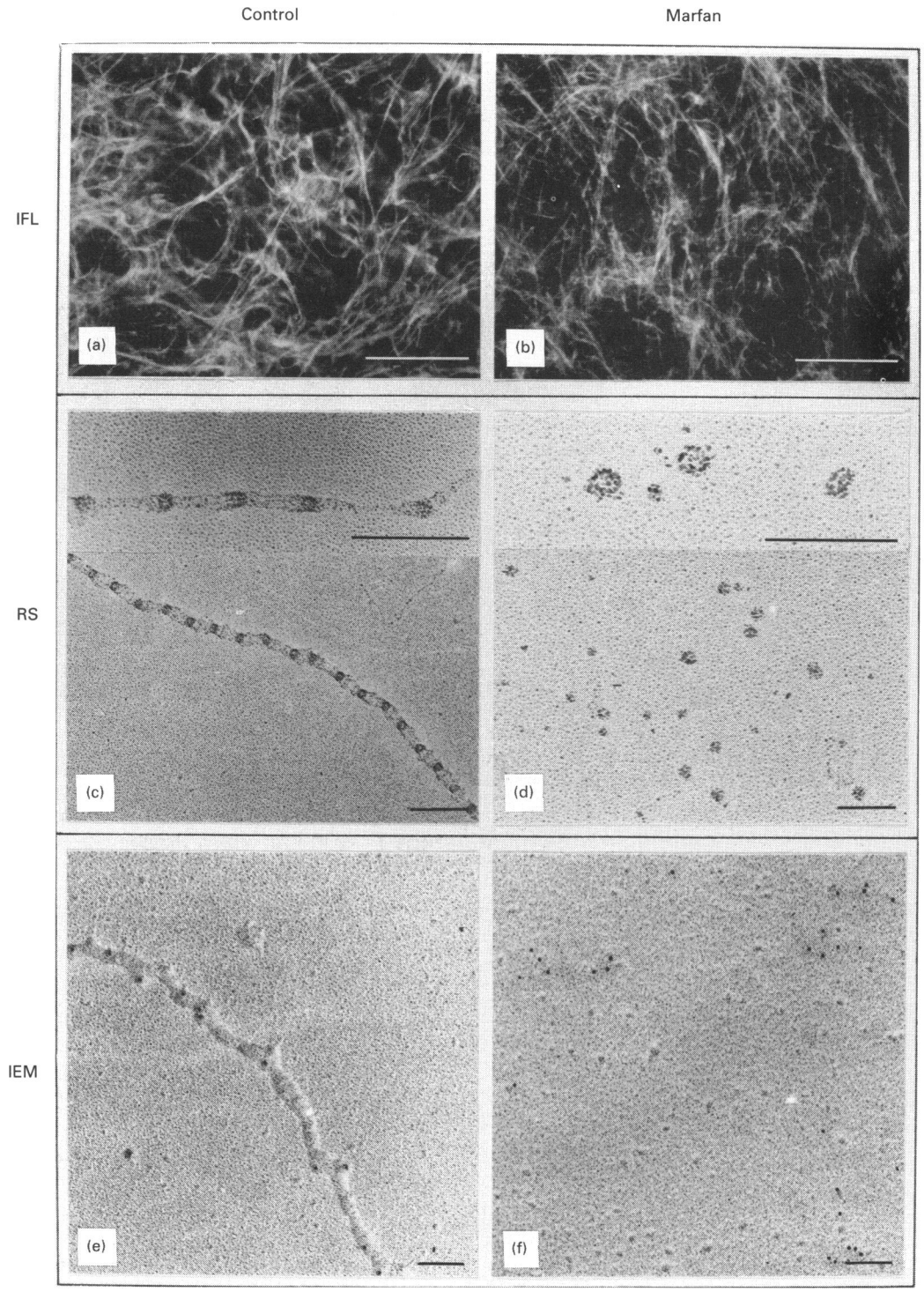

Figure 8 Morphology of microfibrils elaborated by normal and MFS fibroblasts

(**a**) and (**b**): Immunofluorescence (IFL) visualization with anti-Fib (monoclonal antibody F2) of Fib-positive microfibrils accumulated in hyperconfluent fibroblast cultures. The control (**a**) displays a dense network of extended and branching microfibrils, whereas the patient III/4 (**b**) shows a fainter immunofluorescence and reduced calibre of microfibrils. Scale bars = 10 μm. (**c**) and (**d**) and respective insets: Rotary-shadowing EM (RS) of microfibrils isolated from post-confluent cell layers. Fib microfibrils were clearly recognized in controls by their typical beads-on-a-string appearance (**c** and inset). In contast, only numerous beaded domains were detectable in the patient's cells (**d** and inset). The micrographs shown are representative of all fields examined for both cell types. Scale bars = 100 nm. (**e**) and (**f**): Immunogold localization (IEM) using polyclonal antibody 5507 of Fib epitopes on microfibrillar assemblies isolated from the control confirmed their identity (**e**). Fib-immunoreactive aggregates, probably remnants of the beaded domains, but no microfibrils, were detected in the patient (**f**). Scale bars = 100 nm.

microfibrillar pattern as such was unchanged. The intensity of fluorescence, however, appeared to be slightly diminished and the microfibrils appeared to be thinner (Figure 8b).

Examination by rotary-shadowing EM of high-molecular-mass material solubilized from post-confluent bacterial collagenase-solubilized cell layers demonstrated the presence of extensive and abundant microfibrils in control cell layers (Figure 8c). The microfibrils elaborated by control fibroblasts were similar in morphology to those previously isolated from tissues [14,18,19,22]. In marked contrast with the control cultures, in the patient's cell-layer extracts no intact periodic microfibrillar assemblies were demonstrable, although abundant beaded domains were present (Figure 8d).

The identity of microfibrillar assemblies in control extracts was confirmed using immunogold localization of fibrillin epitopes (Figure 8e). Fib-immunoreactive material was also detected in the bead-like elements, the only structures which were morphologically identifiable in the patient's cell-layer extracts (Figure 8f).

DISCUSSION

In order to answer the question of how a mutated *FBN1* genotype is translated into the MFS phenotype, studying Fib on the protein level is mandatory. Metabolic labelling of Fib and its analysis by SDS/PAGE as a possible approach has been only recently established [16,23]. Due to the nature of the Fib mutations investigated so far, i.e. a point mutation ([16]; mutation confirmed afterwards, see [10]) or unknown in other cases [23], only quantitative assessments were possible. The relatively large deletion in *FBN1* in the MFS family studied here together with the improved step-gel procedure [16] allowed us to visualize normal and truncated Fib molecules and to follow their fate in the cells, after secretion into the medium and deposition into the ECM. Intracellularly, only the larger form, proFib, was detectable. The respective amounts of proFib and proFib′ in the mutant cell strains were repeatedly shown to be similar, which was in good accordance with the quantification of *FBN1* transcripts in cultured fibroblasts. In culture medium proFib and proFib′ appeared to be cleaved to Fib and Fib′ respectively.

The ratio of proFib:Fib in the culture medium of control cells in various experiments was variable and ranged from approx. 1:1 to 1:5. This initial ratio remained stable for at least 20 h. After a prolonged chase time the precursor seemed to have finally disappeared.

This precursor–product relationship was clearer to judge in the ECM. proFib was consistently the predominant molecule in early chase times 0 and 0.5 h, but was reduced in favour of Fib after 1 h and almost completely cleared at the latest after 4 h of chase. The same occurred principally in the mutant cell strains but initial deposition of proFib appeared to be markedly reduced and the clearance of proFib from the ECM during chase to be faster. The truncated proFib′ was difficult to detect and was obvious only in the experiment with a stronger pulse and only at the 0.5 h chase time point. When we added 0.01% dextran sulphate to the chase medium, we could increase the amounts of both forms extractable from the ECM of control and patients' cells. The striking effect of dextran sulphate was evident after a 1 h chase, where visibility of the truncated proFib was retained. Thus we could demonstrate incorporation of the shortened proFib molecules into the ECM by SDS/PAGE. We could not extract truncated Fib from the ECM of mutant cells. At present we can only speculate that after trimming of proFib′ to Fib′, the Fib′ was either excluded from further incorporation or assembly into microfibrils, or became unextractable by our procedure, possibly due to abnormally tight cross-linking in the ECM.

It is currently a matter of dispute whether there exists a precursor form 'proFib' (larger than Fib by approx. 30 kDa) which has been suggested earlier because of its co-precipitation with antibodies against Fib [23]. Here, the shortened molecules produced by the mutant cells helped to corroborate the concept of a precursor because in pulse–chase experiments the regular proform had a truncated counterpart. This was particularly evident in the presence of the specific calcium chelator EGTA [24], which largely inhibited the conversion of proFib into Fib and led to an accumulation of proFib and proFib′ in the culture medium of the patient's cells. Simultaneous addition of equimolar $CaCl_2$ abolished the EGTA effect. In view of the failure of all other proteinase inhibitors to cause effects comparable with EGTA, our findings are compatible with the assumption that at least one step in the conversion of proFib into Fib is calcium-dependent. Further work is needed to disclose the underlying mechanism.

Obviously, the cleavage process as such was not disturbed by the large deletion residing in the C-terminal 10% of the molecule (Figure 1, region D). The remaining 265 amino acids C-terminal to the deletion comprise two more epidermal growth factor-like motifs (82 residues) and finally the cysteine-poor C-terminus, region E (Figure 1). Interestingly, three out of 15 potential N-glycosylation sites are concentrated in region E (184 residues, about 22 kDa), whereas the first three regions A–C (447 N-terminal amino acids, about 16% of the total sequence and equivalent to approx. 54 kDa) have none [8,25]. Our observation of a relatively stronger effect of tunicamycin on proFib than on Fib suggests that the putative propeptide removed from Fib is N-glycosylated and would be compatible with the assumption of the propeptide residing in region E, the C-terminus (Figure 1).

The isolation of intact microfibrils from dermal fibroblast cultures allowed direct correlation of biochemical defects and microfibrillar abnormalities. Examination by rotary-shadowing EM of high-molecular-mass-fraction material isolated from cell layers clearly showed that the cell layers of normal dermal fibroblast cultures elaborated abundant and extensive microfibrils. In contrast, the patient's cells had not assembled morphologically identifiable periodic microfibrils, although there was evidence for globular structures which resembled microfibrilllar beaded domains, which were identified immunologically. These observations confirm that in this patient products of the mutant allele are secreted but interfere with normal microfibril formation. One explanation might be that the shortened molecules cannot align correctly to form the intermolecular interactions required to ensure microfibrillar integrity.

On the background that the patients' cells produced and secreted at least 50% normal fibrillin, the failure to detect normal microfibrils in the ECM by rotary-shadowing EM argues for the absence of microfibrils composed of normal molecules only. It needs to be established what the minimal number of mutant Fib molecules is to severely interfere with the integrity of a microfibril. It is likely, that this number is very small, since there is evidence from co-cultivation experiments with normal cells and those from a patient with neonatal MFS that even minimal amounts of mutant Fib molecules can have dramatic consequences for the formation of microfibrils in culture [26].

We are indebted to Dr. Lynn Sakai for the CLM-5 probe for Fib and Dr. Maurice Godfrey for monoclonal antibody F2 to Fib. We appreciate the excellent photographic and art work by L. Burger and Susanne Staubli and the Cytogenetics Unit at St. George's for their invaluable help with the cell cultures. We gratefully acknowledge the financial support of the European Concerted Action on Heritable Connective Tissue Disorders 1990–1992 in general and in particular that of the British Heart

Foundation, Marfan Trust, British Marfan Association (A.C.) and the Wellcome Trust (C.M.K.), The Academy of Finland (L.P. and K.K.), and the Swiss National Foundation (grant 32-27884.89/2; B.S. and M.R.). Part of this work was presented at the 2nd International Marfan Symposium in San Francisco, November 1992, with generous support of the Swiss Marfan Foundation.

REFERENCES

1 Pyeritz, R. E. (1993) in Connective Tissue and Its Heritable Disorders. Molecular, Genetic, and Medical Aspects (Royce, P. and Steinmann, B., eds.), pp. 437–468, Wiley–Liss, New York
2 Sakai, L. Y., Keene, D. R. and Engvall, E. (1986) J. Cell Biol. **103**, 2499–2509
3 Hollister, D. W., Godfrey, M., Sakai, L. Y., and Pyeritz, R. E. (1990) N. Engl. J. Med. **323**, 152–159
4 Kainulainen, K., Pulkkinen, L., Savolainen, A., Kaitila, I. and Peltonen, L. (1990) N. Engl. J. Med. **323**, 935–939
5 Lee, B., Godfrey, M., Vitale, E., Hori, H., Mattei, M.-G., Sarfarazi, M., Tsipouras, P., Ramirez, F. and Hollister, D. W. (1991) Nature (London) **352**, 330–334
6 Magenis R. E., Maslen, C. L., Smith, L., Allen, M. and Sakai, L. Y. (1991) Genomics **11**, 346–351
7 Dietz, H. C., Cutting, G. R., Pyeritz, R. E., Maslen, C. L., Sakai, L. Y., Corson, G. M., Puffenberger, E. G., Hamosh, A., Nanthakumar, E., Curristin, S. M., Stetten, G., Meyers, D. A. and Francomano, C. A. (1991) Nature (London) **352**, 337–339
8 Pereira, L., D'Alessio, M., Ramirez, F., Lynch, J. R., Sykes, B., Pangilinan, Th. and Bonadio, J. (1993) Hum. Mol. Genet. **2**, 961–968
9 Kainulainen, K., Sakai, L. Y., Child, A., Pope, F. M., Puhaka, L., Ryhänen, L., Palotie, A., Kaitila, I. and Peltonen, L. (1992) Proc. Natl. Acad. Sci. U.S.A. **89**, 5917–5921
10 Kainulainen, K., Karttunen, L., Puhakka, L., Sakai, L. and Peltonen, L. (1994) Nature Genet. **6**, 64–69
11 Godfrey, M., Vandemark, N., Wang, M., Velinov, M., Wargowski, D., Tsipouras, P., Han, J., Becker, J., Robertson, W., Droste, S. and Rao, V. H. (1993) Am. J. Hum. Genet. **53**, 472–480
12 Dietz, H. C., Valle, D., Francomano, C. A., Kendzior, R. J., Pyeritz, R. E. and Cutting, G. R. (1993) Science **259**, 680–682
13 Chirgwin, J. M., Przybala, A. E., MacDonald, R. J. and Rutter, W. J. (1979) Biochemistry **18**, 5294–5299
14 Shuttleworth, C. A., Berry, L. and Kielty, C. M. (1992) Arch. Oral Biol. **37**, 1079–1084
15 Laemmli, U. K. (1970) Nature (London) **227**, 680–685
16 Raghunath, M., Superti-Furga, A., Godfrey, M. and Steinmann, B. (1993) Hum. Genet. **90**, 511–515
17 Laskey, R. A. and Mills, A. D. (1975) Eur. J. Biochem. **56**, 335–341
18 Kielty, C. M., Cummings, C., Whittaker, S. P., Shuttleworth, C. A. and Grant, M. E. (1991) J. Cell Sci. **99**, 797–807
19 Kielty, C. M., Berry, L., Whittaker S. P. and Shuttleworth, C. A. (1993) Matrix **13**, 103–112
20 Waggett, A. D., Kielty, C. M. and Shuttleworth, C. A. (1993) Ann. Rheum. Dis. **52**, 449–453
21 Lazarides, E. and Granger, B. L. (1982) Methods Enzymol. **85B**, 488–510
22 Kielty, C. M. and Shuttleworth, C. A. (1993) J. Cell Sci. **106**, 167–173
23 McGookey Milewicz, D., Pyeritz, R. E., Crawford, E. S. and Byers, P. H. (1992) J. Clin. Invest. **89**, 79–86
24 Harrison, S. M. and Bers, D. M. (1987) Biochim. Biophys. Acta **925**, 133–143
25 Corson, G. M., Chalberg, S. C., Dietz, H. C., Charbonneau, N. L. and Sakai, L. (1993) Genomics **17**, 476–484
26 Raghunath, M., Godfrey, M. and Steinmann, B. (1993) Am. J. Med. Genet. **47**, 156

Received 16 December 1993/7 April 1994; accepted 19 April 1994